Medical Engineering and Physics 74 (2019) 23–32

Contents lists available at ScienceDirect

Medical Engineering and Physics

journal homepage: www.elsevier.com/locate/medengphy

Estimation of pulsatile cerebral arterial blood volume based on transcranial doppler signals

Leanne A. Calviello[a,*], Frederick A. Zeiler[b,c,d], Joseph Donnelly[a], Agnieszka Uryga[e], Nicolás de Riva[f], Peter Smielewski[a], Marek Czosnyka[a]

[a] Division of Neurosurgery, Department of Clinical Neurosciences, Addenbrooke's Hospital, University of Cambridge, United Kingdom
[b] Division of Anesthetics, Addenbrooke's Hospital, University of Cambridge, Cambridge, United Kingdom
[c] Section of Neurosurgery, Department of Surgery, University of Manitoba, Winnipeg, Canada
[d] Clinician Investigator Program, University of Manitoba, Winnipeg, Canada
[e] Department of Biomedical Engineering, Faculty of Fundamental Problems of Technology, Wroclaw University of Science and Technology, Wroclaw, Poland
[f] Neuroanesthesia Division, Anesthesiology Department, Hospital Clinic, Universitat de Barcelona, Barcelona, Spain

ARTICLE INFO

Article history:
Received 9 January 2019
Revised 30 June 2019
Accepted 28 July 2019

Keywords:
Neurocritical care
Traumatic brain injury
Spectral pulsatility index
Cerebral arterial blood volume
Transcranial doppler

ABSTRACT

Objective: Mathematical modeling of cerebral hemodynamics by descriptive equations can estimate the underlying pulsatile component of cerebral arterial blood volume (CaBV). This way, clinical monitoring of changes in cerebral compartmental compliances becomes possible. Our aim is to validate the most adequate method of CaBV estimation in neurocritical care.

Approach: We retrospectively reviewed patients with severe traumatic brain injury (TBI) [admitted from 1992–2012] and continuous transcranial Doppler (TCD) monitoring of cerebral blood flow velocity (FV) displaying either plateau waves of intracranial pressure (ICP), episodes of controlled, mild hypocapnia, or vasopressor-induced increases in arterial blood pressure (ABP). Each cohort was analyzed with continuous flow forward (CFF, pulsatile blood inflow and steady blood outflow) or pulsatile flow forward (PFF, both blood inflow and outflow are pulsatile) modeling approaches for estimating the pulse component of CaBV. Spectral pulsatility index (sPI, the first harmonic of the FV pulse/mean FV) can be estimated using the compliance of the vascular bed (Ca) and the cerebrovascular resistance (CVR – here, Ra). We compared three possible methods of assessing Ca (C1: the CFF model, C2 and C3: the PFF models based on ABP or cerebral perfusion pressure (CPP) pulsations, respectively) and combined them with three possible methods of assessing Ra (Ra1= ABP/FV, Ra2= the resistance area product, and Ra3= CPP/FV). Linear regression techniques were applied to describe the strength of each CaBV estimator (a combination of Ca and Ra) against sPI.

Main Results: The combination of C1 and Ra3 (PI_C1Ra3) was the superior descriptor of CaBV as approximated by sPI for both the plateau waves and the hypocapnia cohorts ($r = 0.915$ and $r = 0.955$, respectively). The combination of C1 and Ra1 (PI_C1Ra1) was nearly as robust in the vasopressors cohort ($r = 0.938$ and $r = 0.931$, respectively).

Significance: TCD-based estimation of CaBV pulsations seems to be feasible when employing the CFF modeling approach.

Abbreviations: ABP, arterial blood pressure; Ca, compliance of the vascular bed; CaBV, cerebral arterial blood volume; ΔCaBV, change in cerebral arterial blood volume; CBF, cerebral blood flow; CFF, continuous flow forward model (pulsatile blood inflow and steady blood outflow); Ci, compliance of the cerebrospinal space; CPP, cerebral perfusion pressure; CrCP, critical closing pressure; FV, flow velocity; ICP, intracranial pressure; MCA, middle cerebral artery; PFF, pulsatile flow forward model (both blood inflow and outflow are pulsatile); Ra, cerebrovascular resistance; sPI, spectral pulsatility index (the first harmonic of the FV pulse/mean FV; tau (τ), cerebrovascular time constant; TBI, traumatic brain injury; TCD, transcranial Doppler ultrasonography.

* Corresponding author.
E-mail addresses: lac76@cam.ac.uk (L.A. Calviello), umzeiler@myumanitoba.ca (F.A. Zeiler), agnieszka.uryga@pwr.edu.pl (A. Uryga), nderiva@clinic.cat (N. de Riva), ps10011@cam.ac.uk (P. Smielewski), mc141@medschl.cam.ac.uk (M. Czosnyka).

https://doi.org/10.1016/j.medengphy.2019.07.019
1350-4533/

1. Introduction

The volume of arterial blood circulating throughout the brain at any one time can be adversely affected by traumatic brain injury (TBI). Pulsatile cerebral arterial blood volume (CaBV) can now be modeled with different input signals. Although this modeling reflects the inherent nature of blood flow throughout the brain, there is no consensus on which specific combination of model elements yields a best-fit equation that could be globally applied in neurocritical care. The purpose of this specific study is to tease apart the extant modeling methods themselves [1–7] with the following aims: (a) to comprehend which method is most suitable for describing patient hemodynamics, and (b) to build a function able to monitor changes in cerebral compartmental compliances when considered alongside invasive monitoring and data-driven trend charts.

1.1. Fundamentals of mathematical modeling

We concentrate on building mathematical models of cerebral circulation able to account for pulsatile changes in the vasculature as a result of the cardiac cycle. Transcranial Doppler ultrasonography (TCD) can both capture and continuously monitor cerebral hemodynamic changes in real time; cerebral blood flow velocity (FV) through the middle cerebral artery (MCA) can be expressed as a variable that can be further analyzed with ICM+^{TM} software to provide additional descriptors of hemodynamic activity.

With this application, Kim et al. [1] studied the changes in compartmental compliances (volume/pressure ratios expressed as either: Ca – the compliance of the cerebral arterial bed or Ci – the compliance of the cerebrospinal space) during plateau waves of ICP. During this event, the Ca and Ci compartments of the brain vary inversely as a result of dynamic shifts in the vasomotor tone of the cerebral vessels [1]. These authors [1] emphasized the mean arterial inflow curve when computing a comprehensive descriptor of pulsatile cerebral arterial blood volume and their model below [1] returns the TCD-derived parameter *CaBV*. This parameter can be mathematically transformed through Fourier analysis to yield the fundamental harmonics of pulsatile components of CaBV, allowing a further-detailed expression of cerebral hemodynamics:

$$CaBV(n) = S_a \times \sum_{i=m_1}^{m_n} [CBFVa(i) - mean(CBFVa)]\Delta t \ (i) \quad (1)$$

where: S_a represents the cross-sectional area of the MCA, m_1 the first sample of the interval, n the number of samples, *CBFVa* the cerebral arterial blood flow velocity, and Δt is the time interval between two consecutive samples [1].

The foundations of this present study are rooted in the outcomes from experimental modeling research conducted by Uryga et al. [7]. While manipulating arterial blood carbon dioxide concentration in healthy volunteers, the authors [7] compared the abilities of continuous flow forward (CFF) and pulsatile flow forward (PFF) models of pulsatile CaBV change as holistic descriptors of various cerebral hemodynamic indices. “Flow forward” refers to the direction of cerebral blood transport from large arteries into resistive arterioles. The CFF modeling approach relies on the balance between the simultaneously-opposing forces of pulsatile cerebral blood inflow and cerebral blood outflow, which influence changes in CaBV. Citing Avezaat and van Eijndhoven (1986) [8], they created a time-integrated function of the difference between both inflow and outflow over a single cardiac cycle (Eq. (2), below).

$$\Delta C_a BV_{CFF}(t) = \int_{t_0}^{t} (CBF_a(s) - meanCBF_a)ds \quad (2)$$

However, when employing TCD, this simplistic function requires averaging over several cardiac cycles to provide a surrogate measure of the blood inflow and outflow that occur in tandem [7,9]. To counter the effects of the variability of both blood outflow and systemic vascular impedances as a result of pulsatile changes in the ABP waveform, a second modeling approach was necessitated, becoming PFF. CaBV expressed by PFF would be a time-integrated function of the difference between the cerebral blood flow (CBF) signal and the ABP signal divided by CVR. The CVR can be estimated by TCD (i.e. the ratio between mean ABP and CBF, normalized by the unknown cross-sectional area of the MCA, which is presumed constant, see Eq. (3), below). Uryga et al. [7] reported that each model’s virtual signal is able to capture the pulsatile nature of its constituents and is respectively identified by their different waveform shapes and amplitudes.

$$\Delta C_a BV(t)_{PFF} = \int_{t_0}^{t} \left(CBF_a(s) - \frac{ABP(s)}{CVR} \right) ds \quad (3)$$

where: s – the arbitrary time variable of integration, CBF_a– cerebral blood flow velocity, *ABP* – arterial blood pressure, and *CVR* – cerebrovascular resistance [7].

Our study modifies the PFF modeling approach in particular to include both ABP and cerebral perfusion pressure (CPP), and to consider both CFF and PFF as potentially useful tools in the determination of clinical outcome. The previous method of CaBV modeling assumed constant outflow of the blood from the modeled compartment (compliance of cerebral arteries and vascular resistance). Our proposed modification (PFF) presumes that outflow may be pulsatile, and investigates changes in formulas for the calculation of the amplitude of CaBV estimators.

To our knowledge, this paper is the first of its kind attempting to apply these modeling perspectives to a population of neurocritically ill patients.

2. Methods

2.1. Patients

We performed a retrospective review of 52 adult patients selected from a database of 432 moderately to severely head-injured patients stored between 1992 and 2012 that demonstrated a variety of clinically-extreme scenarios. Of these 52 patient datasets: 16 presented plateau waves of ICP which are difficult to capture during routine TCD monitoring sessions [10], 19 underwent a period of mild, controlled hypocapnia (30–60 minutes’ duration), and 17 received vasopressors to stabilize mean ABP that fluctuated at least 15 mm Hg during the recording. All patients were admitted to the Neurosciences Critical Care Unit (NCCU) at Addenbrooke’s Hospital, Cambridge, United Kingdom. All patients were sedated and mechanically ventilated; barring the hypocapnic challenge to assess CO_2 reactivity, all patients were treated in accordance with a ICP/CPP-oriented protocol that constrained ICP below 20–25 mm Hg and maintained CPP between 60–70 mm Hg [11,12]. CPP was calculated as the difference between ABP and ICP. Table 1 describes these patients in detail.

Our interest in these particular patient groups rests in the observation of the direction(s) of CaBV changes in response to biophysical “challenges” [11–19], which are thought to mimic physiological responses to hemodynamic disturbances that are provoked, pathological, or pharmacological. Therefore, CaBV can be manipulated by ICP [11,13,14], CO_2 [12,15–17], and ABP [18–20], making these parameters important clinical discriminants. Dramatic fluctuations in pulsatile CaBV can be best studied in patients exhibiting complex clinical profiles, such as plateau waves of ICP, hypocapnia, and unstable ABP; these specific patient cohorts were chosen to test the veritable limits of mathematical modeling of cerebral hemodynamics, and to provide secondary insight into outcome prediction.

Table 1
Patient demographics and outcomes.

Patient Cohort	Number of Patients	Mean Age (years)	Male:Female Ratio	Median Admission GCS	Glasgow Outcome Scale at Discharge	
Plateau Waves	16 (5/16 lost to follow-up)	27.18 (range: 17 to 32)	12:4	5 (range: 1 to 10)	*GOS*	*# of Patients*
					Dead	0
					PVS	4
					Severe disability	5
					Moderate disability	0
					Good	2 N.A.: 5
Hypocapnia	19 (4/19 lost to follow-up)	39.1 = 38 (range: 17 to 70)	14:5	6 (range: 3 to 12)	*GOS*	*# of Patients*
					Dead	1
					PVS	0
					Severe disability	5
					Moderate disability	8
					Good	1 N.A.: 4
Vasopressors	17 (5/17 lost to follow-up)	32.79 (range: 18 to 69)	13:4	5 (range: 3 to 9)	*GOS*	*# of Patients*
					Dead	2
					PVS	0
					Severe disability	2
					Moderate disability	4
					Good	4 N.A.: 5

GCS = Glasgow Coma Scale, GOS = Glasgow Outcome Scale, # = number, PVS – persistent vegetative state.

Retrospective data was anonymized and is stored as such in our NCCU Users Group database. TCD recordings were incorporated into standard patient monitoring practices on the NCCU and utilized an anonymized database of physiological monitoring variables in neurocritical care. Demographic data, injury severity, and clinical status at hospital discharge were collected prospectively during the monitoring of these patients; these clinical records were not consulted further to provide additional information for this study. All data retrieved from the database was extracted from these pre-existing patient records, and fully anonymized. Data pertaining to long-term outcome or patient-identifiers was not available, and formal patient or proxy consent to access these items was not sought, with the exception of the vasopressors cohort, which consented for positron emission tomography (PET) under two different blood pressure levels.

2.1.1. ICP plateau waves

The observable phenomenon of an ICP plateau wave has been explained as a function of increasing CaBV at the expense of cerebral vasomotor tone and flow regulatory mechanisms [15]. As cerebral vessels react with maximal dilation and obstruct draining veins, both the velocity and the volume of blood flowing within their walls increases. However, the brain cannot accommodate these alterations as they occur, so ICP rapidly increases. The increased amplitude of the raw ICP waveforms is accompanied by increased ICP, and can be attributed to the influx of pulsatile cerebral blood coursing through the cerebral vessels, as a product of both ABP and CVR as opposed to solely an increase in mean ICP [13,21]. Both CFF and PFF models can express the heightened magnitude of pulsatile changes in CaBV as a result of ICP plateau waves. It was hypothesized that this cohort in particular would be best-described by the PFF model using CPP as input, as plateau waves increase ICP, and therefore will affect CPP.

2.1.2. Hypocapnia

Data from patients submitted to short-term episodes of hypocapnia (mean $PaCO_2$, the partial pressure of carbon dioxide in arterial blood, was maintained at 4.38±0.34 kPa and deviated on average by 0.72±0.26 kPa during hypocapnia) were also included to test the limits of ΔCaBV modeling in the opposite direction. The vasoconstrictive effects of hypocapnia can be observed in the characteristic reduction of ICP attributed to a "backshift of the working point on [the] pressure-volume curve", in which ΔCaBV circulation is negatively affected by the increasing resistance to arterial inflow [18]. Cerebral autoregulation is thus compromised [22]; prolonged exposure to hypocapnia exacerbates the risk of both disability and mortality, as decreasing ICP at the expense of CPP overreaching its targeted value can lead to ischemia or irreversible damage to brain tissue [17].

2.1.3. Vasopressors

Infusions of vasopressors such as norepinephrine or phenylephrine have been found to increase cerebral perfusion and oxygenation in both human and swine models [23]. Following TBI, they are administered to increase ABP and CPP to prevent secondary ischemia [20,24]. Our selected cohort of patients maintained a mean ABP of 87.31±7.16 mm Hg that was increased to 111.41±6.45 mm Hg following infusion of either phenylephrine (0.5 mcg/kg/min) or norepinephrine (0.05 mcg/kg/min). We hypothesized that both PFF models, either with ABP or CPP used as input, would be strongly correlated with this cohort.

2.2. Monitoring

All patients received both invasive and non-invasive monitoring while under clinical observation. Raw data signals from select monitoring devices were captured and archived electronically through WREC software (Warsaw University of Technology) or ICM+™ (licensed through Cambridge Enterprise, Cambridge, U.K.; http://www.neurosurg.cam.ac.uk/icmplus).

ABP was continuously monitored invasively [from the radial artery using a pressure monitoring kit (Baxter Healthcare C.A., U.S.A.; Sidcup, U.K.)]. ICP was monitored using an intraparenchymal probe with strain gauge sensors (Codman & Shurtleff, M.A., U.S.A.). End-tidal CO_2 ($ETCO_2$) was measured in the patients experiencing periods of mild, controlled hypocapnia via capnograph (Marquette Solar 8000 M, GE Medical Systems, U.K.). Cerebral blood flow velocity (FV) was recorded from both unilateral and bilateral monitoring of the middle cerebral artery (MCA) with a 2 MHz TCD probe (Multi Dop X4, DWL Elektronische Systeme, Sipplingen, Germany). Data were processed through a 16-bit, 100 kHz analog-to-digital converter (DT9803 USB Data Acquisition (DAQ) Module, Measurement Computing Corporation, Norton, M.A., U.S.A.).

Raw TCD data sampled from the three types of events (ICP plateau waves, hypocapnia, and vasopressors) included in the study encapsulated the baseline readings, the entirety of the challenge/event, and the post-event recordings. Signal artifact removal was achieved manually. CPP was determined from the difference

between raw ABP and ICP signals. The average duration of these TCD recordings was over 108.59±57.56 minutes, with a minimum of 18 minutes and maximum of 177 minutes captured per patient. 18–90 minutes of continuous TCD data recordings were obtained from the plateau waves cohort, with 85–138 and 135–177 minutes each obtained from the hypocapnia and vasopressors cohorts, respectively.

2.3. Data processing

Our previous study [10,25] allowed the expression of TCD-based "spectral pulsatility index" (sPI), defined above as sPI = F1/FVm) using the following model presented below in Eq. (4). This model describes the relationships among several cerebral hemodynamic parameters that would be expected to yield variations in CPP [10]. Generally, our present task is to choose estimators for Ca and ΔCaBV, which produce the best agreement between the left and right sides of this equation.

$$sPI = \frac{A_1}{CPP_m} \times \sqrt{(CVR \times Ca)^2 \times HR^2 \times (2\pi)^2 + 1} \tag{4}$$

where A_1 represents the fundamental harmonic of the ABP pulse waveform determined using Fourier transform, *Ca* the cerebral arterial compliance, CPP_m the calculated mean of recorded CPP values, *CVR* the cerebrovascular resistance, and *HR* the heart rate calculated in Hz [25]. All parameters were calculated as averages over a 10-second time window.

Within ICM+™, virtual signals from the invasive monitoring (ABP and ICP) devices and from TCD blood flow velocity monitoring (FV) were sampled at a frequency of 50 Hz to form the backbones of the three CaBV change approximation models. A continuous flow forward model (CFF) [5,7,8,26] was applied as a time-integral of FV to form $\Delta CaBV_{CFF}$ ($CaBV_1$; Eq. (5)) sampled at a frequency of 50 Hz (Eq. (5)), whereas the two pulsatile flow forward models (PFF_{ABP} and PFF_{CPP}) were similarly derived using ABP and CPP as input, to form the respective $\Delta CaBV_{PFF_{ABP}}$ ($CaBV_2$; Eq. (6)) and $\Delta CaBV_{PFF_{CPP}}$ ($CaBV_3$; Eq. (7)).

$$\Delta CaBV_{CFF}(t) = \int_{to}^{t} (FV(i) - FV_m)\, di \tag{5}$$

$$\Delta CaBV_{PFF_{ABP}}(t) = \int_{to}^{t} \left(FV(i) - \left(\frac{ABP_{(i)}}{\frac{ABPm}{FVm}} \right) di \right. \tag{6}$$

$$\Delta CaBV_{PFF_{CPP}}(t) = \int_{to}^{t} \left(FV(i) \left(\frac{ABP_{(i)} - ICP_{(i)}}{\frac{ABPm - ICPm}{FVm}} \right) \right) - ds \tag{7}$$

where: t_0 and t are the respective beginning and end of a single cardiac cycle, Δt is the time interval between two consecutive samples, $FV(i)$, $ABP(i)$, *and* $ICP(i)$ are the moving averages of FV, ABP, and ICP over a specified time window including previous cardiac cycles (a moving average filter of 600 seconds was applied), *FVm* is the mean value of FV, *ABPm* is the mean value of ABP, *ICPm* is the mean value of ICP, and *s* is the arbitrary variable of integration.

Primary analysis involved the determination of time-averaged mean values for ABP, CPP, FV, ICP, $\Delta CaBV_1$, $\Delta CaBV_2$, and $\Delta CaBV_3$. Each mean was calculated during 10-second time windows and continuously updated every 10 seconds. For the CFF model, Fourier transform was employed to determine the fundamental frequencies of each of the above parameters, to use as scaffolds for more extensive evaluation of spectral changes in ΔCaBV, yielding $AmpCaBV_{CFF}$. For the PFF models, we instead calculated the fundamental amplitudes with Eq. (8) (see Appendix A); $AmpCaBV_{PFF_{CPP}}$ was obtained with this same formula but required AmpCPP as input rather than AmpABP (see Appendix A). Each of these calculations was similarly sampled and updated over a 10-second time window.

The secondary phase of analysis computed time-averaged mean values of all of the above parameters, sampled and updated over a 10-second time window, with the introduction of time-averaged mean values of $\Delta CABV_1$, $\Delta CABV_2$, and $\Delta CABV_3$ resolved into the spectral domain to yield the respective $CABV_{1S}$, $CABV_{2S}$, and $CABV_{3S}$. These spectral components were included in the final analysis to create nine separate models of CaBV approximation to be validated against the existing sPI model [10,25] describing changes in CPP as a result of extreme pathology that were directly observed by TCD.

Final data processing efforts continued to determine the time-averaged mean values from previous analytic phases, each sampled and updated over a 10-second time window. Several new derived parameters were introduced here, including: sPI as the quotient of the means of F1 and FV, mean $CABV_{1S}$, $CABV_{2S}$, and $CABV_{3S}$, and the time constant of the cerebral arterial bed (tau, τ). Commonly interpreted as a simplified electronic circuit model consisting of a single resistor and capacitor, τ is evaluated as the relative time period required to fill the cerebral arterial bed [5,7]. τ is the product of Ca and CVR, and emphasizes the "mutual interdependence" of these parameters from an absolute value of ABP [27,28]. Additionally, τ is not affected by the surface area of the middle cerebral artery (MCA), so challenges to the long-held assumption of its constant value do not pose a threat to this parameter's applicability to patient data.

Although the calculation of τ was not the primary feature of this report, its inclusion in the final analysis supports its utility for further description of changes in pulsatile CaBV. τ varies inversely with fluctuations in ABP or CPP, which are crucial components of our interpretation of CFF and PFF models [27,28]. Our nine derived estimators of CaBV pulsatility each employ a similar circuit model to τ, with single resistors (Ra1-Ra3) and capacitors represented by manipulated combinations of aspects of either the continuous or the pulsatile flow forward models and cerebral hemodynamic parameters (ABP, CPP, FV) sourced through ICM+™. The resistors and capacitors "available" (listed as PI_CxRax) for the creation of each of these models are listed below, with the full formulaic characterizations to be found in Appendix B.

All data post-processing was exported from each patient to separate comma-separated variable (CSV) files for further statistical analysis.

2.4. Statistics

All statistical analyses were conducted utilizing R (R Core Team [2017]; R: a language and environment for statistical computing. R Foundation for Statistical Computing, Vienna, Austria. URL https://www.R-project.org/). Post-processing, individual CSV documents containing the data of each patient, were compiled into one CSV document per cohort containing the relevant patients and all of the signals described above. Cerebral hemodynamic trends were separately analyzed for each of the three patient cohorts (as plateau waves, hypocapnia, and vasopressors) to appreciate the physiological differences between clinical profiles. A visual example of the trends exhibited by a patient from each group was exported from ICM+™, provided in Fig. 1 below.

Various statistical techniques were employed to describe the strength of the following relationships in all three patient cohorts: sPI vs. PI_C1Ra1, PI_C1Ra2, PI_C1Ra3, PI_C2Ra1, PI_C2Ra2, PI_C2Ra3, PI_C3Ra1, PI_C3Ra2, and PI_C3Ra3. Goodness of fit between the metric of sPI and each of the nine ΔCaBV estimator models was assessed via linear regression in R; this was achieved with the Pearson correlation coefficient (r) and the determination coefficient (R^2).

The Bland Altman method was applied, also in R, to measure the agreement between sPI and each respective estimator model

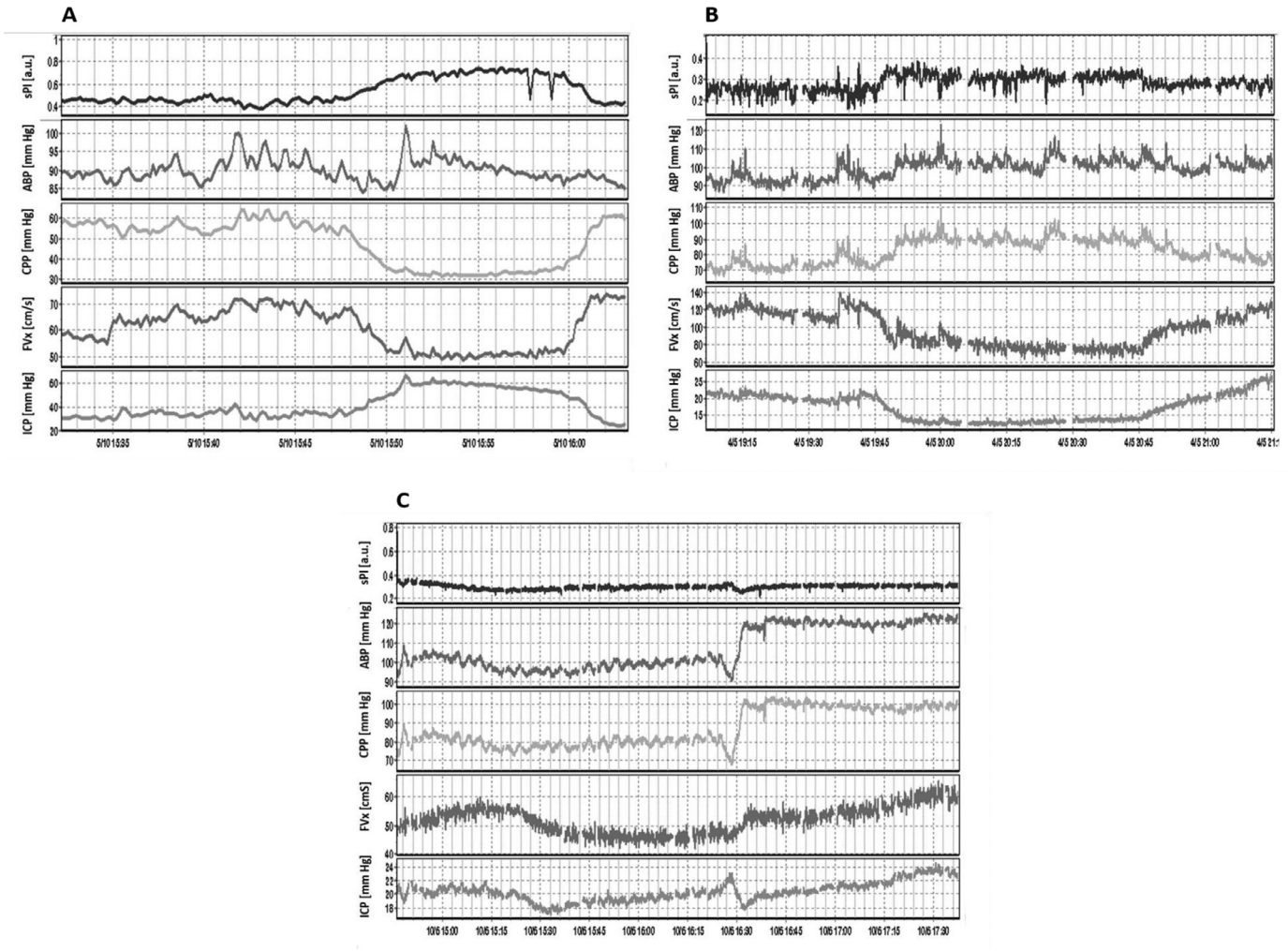

Fig. 1. Examples of sPI, ABP, CPP, FV, and ICP dynamic trends exported directly from ICM+™ for a single patient in the (A) plateau waves, (B) mild hypocapnia, and (C) vasopressors cohorts. *sPI*- spectral pulsatility index, *ABP*- arterial blood pressure, *CPP*- cerebral perfusion pressure, *FV*- flow velocity, *ICP*- intracranial pressure, *mm Hg*- millimeters of mercury.

Table 2
sPI vs. Derived PI models in the plateau waves cohort.

	sPI	PI_C1Ra1	PI_C1Ra2	PI_C1Ra3	PI_C2Ra1	PI_C2Ra2	PI_C2Ra3	PI_C3Ra1	PI_C3Ra2	PI_C3Ra3
Entire Recording										
Mean	0.340	0.639	0.369	0.448	0.459	0.326	0.343	0.428	0.325	0.329
Standard Deviation	0.176	0.392	0.119	0.147	0.311	0.182	0.134	0.281	0.212	0.128
Bland Altman Mean	–	−0.299	−0.028	−0.084	−0.119	0.014	−0.002	−0.088	−0.015	0.012
Bland Altman Critical Difference	–	0.548	0.337	0.17	0.506	0.538	0.306	0.501	0.610	0.333
Pearson Correlation Coefficient	–	0.888	0.843	0.915	0.886	0.888	0.889	0.887	0.882	0.886

for the purpose of explaining changes in pulsatile CaBV demonstrated by each pathology. Descriptive statistics for each of the three patient cohorts, along with the results of the linear regression and Bland Altman analyses, are reported in Tables 2–4.

3. Results

3.1. Relationships between sPI and CaBV estimators

Tables 2 (plateau waves), 3 (hypocapnia), and 4 (vasopressors) summarize the mean values and standard deviations of sPI and of the estimator models; they additionally feature summary statistics data for all TCD recordings comprising each of the patient cohorts, and Bland Altman means and critical differences for sPI and each estimator model. To appreciate the agreement between the sPI and each estimator model, the Pearson correlation coefficients (r) were also listed per respective cohort.

The results of the final analyses indicated that irrespective of the patient cohort, each of the nine ΔCaBV estimator models was robustly correlated with sPI. However, the best-fit estimator model that was superior in approximating changes in pulsatile CaBV throughout the entire recording varied as a result of the distinct clinical profiles of these patients. Tables 2–4 demonstrate these trends.

3.1.1. Plateau waves

This cohort demonstrated high agreement between the derived and the "traditional" parameters comprising the electronic circuit-inspired estimator models. The readings from each subgroup were closely approximated to sPI by all of the models (fully detailed in

Table 3
sPI vs. Derived PI models in the hypocapnia cohort.

	sPI	PI_C1Ra1	PI_C1Ra2	PI_C1Ra3	PI_C2Ra1	PI_C2Ra2	PI_C2Ra3	PI_C3Ra1	PI_C3Ra2	PI_C3Ra3
Entire Recording										
Mean	0.301	0.432	0.337	0.385	0.273	0.253	0.262	0.265	0.250	0.257
Standard Deviation	0.102	0.150	0.109	0.124	0.094	0.104	0.086	0.087	0.103	0.082
Bland Altman Mean	–	−0.131	−0.036	−0.084	0.029	0.048	0.039	0.036	0.051	0.044
Bland Altman Critical Difference	–	0.117	0.102	0.061	0.065	0.161	0.065	0.068	0.165	0.072
Pearson Correlation Coefficient	–	0.918	0.588	0.955	0.830	0.600	0.821	0.830	0.613	0.815

Table 4
sPI vs. Derived PI models in the vasopressors cohort.

	sPI	PI_C1Ra1	PI_C1Ra2	PI_C1Ra3	PI_C2Ra1	PI_C2Ra2	PI_C2Ra3	PI_C3Ra1	PI_C3Ra2	PI_C3Ra3
Entire Recording										
Mean	0.299	0.484	0.374	0.434	0.324	0.306	0.312	0.314	0.305	0.305
Standard Deviation	0.647	0.710	0.088	0.628	0.714	0.721	0.631	0.715	0.807	0.631
Bland Altman Mean	–	−0.044	−0.075	−0.134	−0.024	−0.006	−0.023	−0.014	−0.005	−0.005
Bland Altman Critical Difference	–	0.072	1.264	0.987	1.099	1.910	1.025	1.104	2.040	1.029
Pearson Correlation Coefficient	–	0.938	0.621	0.931	0.870	0.687	0.826	0.814	0.652	0.781

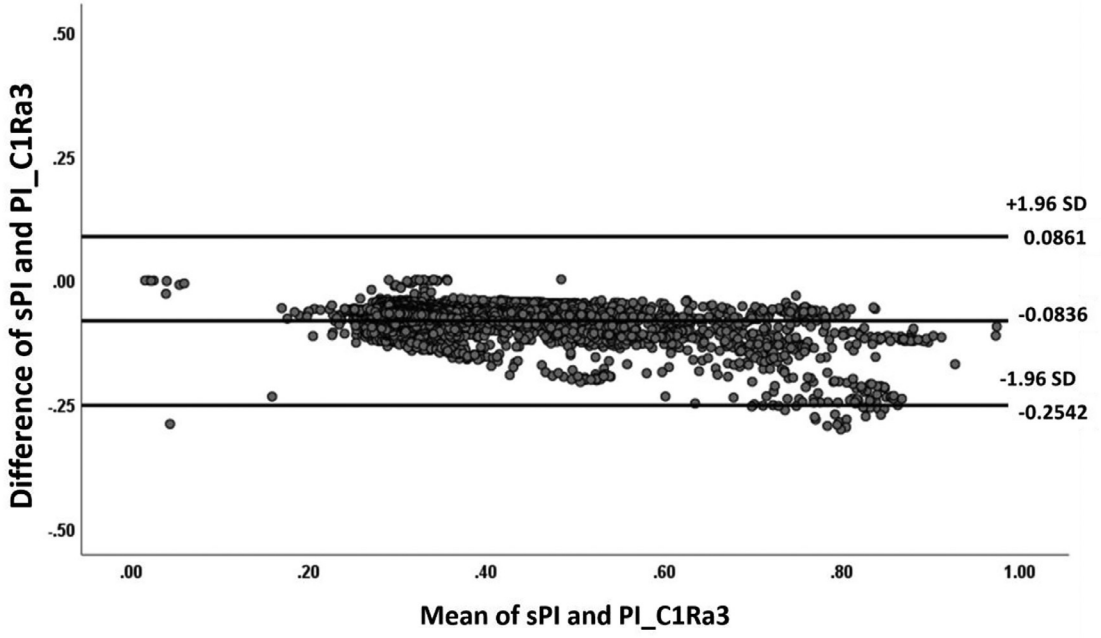

Fig. 2. A Bland Altman plot representing the compatibility between sPI and PI_C1Ra3 to estimate changes in pulsatile CaBV in the plateau waves patient cohort. The bold lines indicate the limits of agreement as measured with a confidence interval of 95%, yielding a bias of −0.0836.

Appendix A), but were most strongly determined by PI_C1Ra3 with an average *r*-value of 0.915 for the entire recording (Fig. 2). The strengths of each estimator as measured against sPI are reported in Table 2, below.

3.1.2. Hypocapnia cohort

The hypocapnia patient cohort provided a similar example of high agreement between parameters determined both invasively and non-invasively. In conjunction with the results from the plateau waves cohort, sPI was closely approximated by all of the models, in particular by PI_C1Ra3 with an average *r*-value of 0.955 for the entire recording (see Table 3, below). PI_C1Ra3 was overwhelmingly found to be the superior estimator of the volumetric changes in cerebral arterial blood within the hypocapnia patient cohort. As above, complete descriptions of each of the models are contained in Appendix A.

3.1.3. Vasopressors cohort

As observed in both the plateau waves and the hypocapnia patient cohorts, the vasopressors cohort also suggested high agreement with sPI. However, when compared to the previous cohorts, the variability between each of the models as predictors of sPI was significantly greater for each recording subgroup, although PI_C1Ra1 and PI_C1Ra3 were repeatedly closely-matched (see Table 4, below). When considering the average *r*-value, the vasopressors patient cohort challenged the notion of PI_C1Ra3 as being considered the "best-fit" for sPI. PI_C1Ra1 and PI_C1Ra3 were nearly identical approximators of sPI, with respective average r-values of 0.938 and 0.931. As above, the construction of each model is outlined in Appendix A.

4. Discussion

The first aim of this study was to assess the feasibility of either a CFF or a PFF model to approximate pulsatile changes in CaBV in physiologically extreme conditions affecting neurocritical care patients. We hypothesized that a PFF model with CPP as the input signal (PI_C3Ra3) would be the best-fit estimator model because its core parameter contains raw signals from both standard

cerebral hemodynamic indices (ABP and ICP) that largely direct patient management. However, our results seem to disprove this hypothesis, suggesting that it is mainly PI_C1Ra3 (closely followed by PI_C1Ra1, but only for the vasopressors cohort – see Tables 2–4) that is the best fit for these groups of neurocritical patients.

Although inspired by the work of Uryga et al. [7] which concluded that PFF was superior to CFF when measured in healthy volunteers during hypo- and hypercapnia, our results taken from a population of TBI patients contradict this point. This could be related to the fact that the CFF method of CaBV estimation is more "stable" for measurement, as it discards the dependence on ABP for calculation that characterizes both PFF modeling scaffolds. ABP appears to be the most sensitive parameter, as any large fluctuations of ABP in patients would dramatically change the value of the numerators of any one of the three resistors applied to either PFF model (please see Appendix A). Though the TCD-based pulsatility index can describe hemodynamic asymmetry and alert clinicians to low CPP, it cannot reliably explain CVR or be considered a secure measure of risk against intracranial hypertension or dysautoregulation [25]. When plotting sPI against CPP [10], the curve does not exhibit an abrupt breakpoint that would indicate the lower limit of autoregulation when targeting CPP in accordance with neurointensive care protocols [9].

We concentrated on building mathematical models of cerebral circulation able to account for pulsatile changes in the vasculature as a result of the cardiac cycle. TCD can capture continuous monitoring of cerebral hemodynamic changes in real time that can be further analyzed with ICM+^{TM} software to provide additional descriptors of hemodynamic activity, such as the compliance of the cerebral arterial bed (Ca) and the cerebrovascular resistance (CVR). Although the diameter of the MCA has been observed as relatively constant in healthy volunteers [29,30] (discounting cases of vasospasm), the volume of cerebral arterial blood flowing through it is subject to change, especially when exposed to extreme physiological conditions (i.e. plateau waves of ICP, hypocapnia, or unstable ABP requiring the use of vasopressors for stabilization) [10].

Although the modeled approximation of ΔCaBV without its venous component appears noncompliant with natural circulatory transit cycles, there is a long-standing assumption that venous flow pulsatility is much lower than its arterial counterpart. Regarding the possible influence of the venous component, Carrera et al. [13] reported that during one cardiac cycle, venous outflow carries a low enough pulsatility to be deemed "negligible" when calculating pulsatile CaBV changes [1,8,9,13,27]. Therefore, ΔCaBV can be represented as the time-integrated difference between the values of current and mean cerebral blood flow velocity [1,13]. In fact, Avezaat and van Eijndhoven [8] had already noted the influence of pulsatile in- and outflow curves in determining the subtle, time-sensitive variations in ΔCaBV that occur over one cardiac cycle. The degree of quantifiable change in pulsatile CaBV would be an effect of the "temporal relationship" between cerebral arterial inflow and venous outflow processes; this is contingent on the impedances of the vascular bed, which can be both actively and passively mediated by either vasomotor tone or compression within the cerebral compartment [8].

4.1. Clinical implications

Improvements in the estimation of ΔCaBV provide various potentially crucial advancements for monitoring critically ill patients. First, in patients suffering from intracranial hypertension, knowledge of which intracranial component is contributing most to ICP elevation is not always clear (i.e. CSF, blood volume, edema, etc.). Optimal models for pulsatile CaBV estimation, such as those presented here, are required to properly outline the blood volume component of ICP. Such knowledge, may allow the implementation of targeted therapies for particular intracranial components contributing to elevated ICP. Second, most clinicians currently manage intracranial hypertension by treating a single number, based on the Brain Trauma Foundation (BTF) guidelines [31]. It is unknown if targeting particular aspects of ICP, such as standard invasively-measured parameters or estimated ΔCaBV, could provide greater impact on patient functional outcome. However, we require adequate, optimized models of ΔCaBV estimation prior to investigating therapies directed at continuously/semi-continuously measured ΔCaBV, we require optimal models of pulsatile CaBV estimation.

Third, we understand that persistent ICP elevations near, or at, the critical closing pressure (CrCP) are detrimental to sustained cerebral blood flow in the setting of brain injury. As accurate CrCP is predicated on cerebral blood volume estimation, it becomes theoretically possible to estimate an individual patient's CrCP in a continuous/semi-continuous manner, allowing clinicians real-time knowledge of this critical threshold that can be incorporated into therapeutic interventions. Fourth, to date, the majority of continuously-measured indices of cerebrovascular reactivity are derived based on the notion that the correlation between slow-wave fluctuations in a surrogate measure of cerebral blood flow (such as TCD-based FV) or ΔCaBV (such as ICP) and a driving pressure (such as ABP or CPP), provide information regarding cerebral autoregulatory status. The most widely employed index, pressure reactivity index (PRx) [5] is based on the correlation between slow-wave fluctuations of ICP (surrogate of CaBV) and mean ABP. In (TBI), PRx has demonstrated a strong association with global outcome [32] and has been validated as a measure of the lower limit of autoregulation in experimental models [33,34]. However, there exists the potential to further optimize our ability to continuously assess cerebrovascular reactivity. With accurate pulsatile CaBV estimation, instead of identifying a surrogate measure of ΔCaBV, such as ICP, we can evaluate more directly vasogenic slow-wave fluctuations in CaBV and their association with either ABP or CPP. Such measures may prove superior to existing measures of cerebrovascular reactivity; however, prior to the evaluation of such measures, one requires optimal models for ΔCBV estimation.

Finally, as both medicine and the critical care management of brain injury patients shift towards a personalized approach, the ability to accurately and continuously assess various aspects of cerebral physiology is of the utmost importance. In TBI care, we've seen the emergence of literature on both individualized CPP [35–37] and ICP [38], based on various aspects of physiologic signal measurement, processing, and analysis. It is unknown where continuously measured ΔCaBV or CrCP will provide additional benefit in such care. However, it isn't until accurate estimation of pulsatile CaBV is provided, that we can begin to evaluate any benefit toward our goal of purely individualized care.

4.2. Limitations

Although a single model could be identified as the most robust estimator of pulsatile CaBV changes when compared against sPI, this study provided only a correlational assessment of model efficacy. Additionally, our proposed model requires numerical integration over sampled signals; this process is prone to errors due to noise. The immediate validity of our study is limited by the common, nearly fundamental assumption that the cross-sectional area of the MCA is of a constant, yet unknown, value. If the MCA is indeed proven variant [39,40], then our calculations would require reconfiguration in order to accommodate for the additional fluctuations in its tone. Our calculations would also be discounted if the negligible contribution of the venous outflow to ΔCaBV calculations is found to be just the opposite; our current models are comprised of time-integrated differences between current and mean cerebral blood flow velocity that make no allowance for ve-

nous outflow during raw signal collection. Our statistical analysis yields such robust agreement among the estimators largely due to their shared parameters with slight mathematical modifications. Further, the patient cohorts selected for this study made up a fraction of the patients within our database; these cohorts were specifically chosen because they represent physiological extremes that would test the limits of the models. Therefore, we assumed that if the models demonstrated such significant effects in these patients, then they should also for the entire database. Finally, of overwhelming significance, is the inability of these TCD-based parameters to provide direct measurements. Despite the power of TCD as a non-invasive predictive tool, each derived parameter contingent on the TCD waveform can only be interpreted as a surrogate descriptor of cerebral hemodynamics. The true value of a TCD-based model (such as PI_C1Ra3) in the determination of pulsatile CaBV changes can only be investigated via comparison with invasive measures, such as PET [17,41,42] or a reference method based on plethysmography (electrical impedance) to attempt to validate alternative techniques.

5. Conclusions

sPI is considered a theoretical explanation of the effects of extreme pathology on CPP [5]. Our results indicated that the CFF-based model of sPI using ICP as an input signal (PI_C1Ra3) performed well within all of the three patient cohorts that we examined; however, this cannot be generalized to the entire population receiving neurocritical care. Further investigation of pulsatile CaBV approximation needs to be conducted in a larger, more heterogenous sample of TBI patients.

Declaration of Competing Interest

MC and PS both have financial interest in a portion of ICM+TM licensing fees.

Funding

MC and PS are both supported by the NIHR Cambridge Biomedical Research Centre and FAZ has received salary support for dedicated research time, during which this project was completed. Such salary support came from: the Cambridge Commonwealth Trust Scholarship, the Royal College of Surgeons of Canada – Harry S. Morton Travelling Fellowship in Surgery and the University of Manitoba Clinician Investigator Program.

Ethical approval

Patient data used for this study was retrospective in nature, and did not require consent or ethical approval for its use. Similar data is collected and processed routinely under the Cambridge University Hospitals NHS Trust NCCU Protocols 29 and 30.

Contributing authors

Frederick A. Zeiler B.Sc. M.D. Ph.D., F.R.C.S.C. (Neurosurgery), Department of Surgery, Rady Faculty of Health Sciences, University of Manitoba

Joseph Donnelly MBChB, Ph.D., Division of Neurosurgery, Dept. of Clinical Neurosciences, University of Cambridge

Agnieszka Uryga, M.Sc. Eng., Department of Biomedical Engineering, Faculty of Fundamental Problems of Technology, Wroclaw University of Technology

Nicolás de Riva, M.D., Division of Neuroanesthesia, Dept. of Anesthesiology, Universitat de Barcelona

Peter Smielewski, Ph.D., Division of Neurosurgery, Dept. of Clinical Neurosciences, University of Cambridge

Marek Czosnyka, Ph.D., Professor of Brain Physics, Division of Neurosurgery, Dept. of Clinical Neurosciences, University of Cambridge

Appendix A. Spectral Models of Cerebral Blood Volume Estimation

$$\begin{array}{ll} \text{Resistors} & \text{Capacitors} \\ \text{Ra1} = \dfrac{ABP_m}{FV_m} & \text{C1} = \dfrac{Amp\,CABV_{CFF}}{Amp\,ABP} \\ \text{Ra2} = \dfrac{A_1}{F_1} & \text{C2} = \dfrac{Amp\,CABV_{PFF_{ABP}}}{Amp\,ABP} \\ \text{Ra3} = \dfrac{CPP_m}{FV_m} & \text{C3} = \dfrac{Amp\,CABV_{PFF_{CPP}}}{Amp\,ABP} \end{array} \tag{8}$$

where ABP_m, CPP_m, and FV_m each represent the mean value of the respective parameter, A_1 the fundamental harmonic of ABP, and F_1 the fundamental amplitude of the FV waveform.

Appendix B. Formulaic Characterizations of Cerebral Arterial Blood Volume Estimator Models

$$\text{PI\_C1Ra1} = \frac{Mean(A_1)}{CPP_m} \times \sqrt{\left(\frac{Mean\ (CABV_{1S})}{Mean\ (A_1)} \times \frac{ABP_m}{FV_m}\right)^2 \times Mean(HrHz)^2 \times (2\pi)^2 + 1}$$

$$\text{PI\_C1Ra2} = \frac{Mean(A_1)}{CPP_m} \times \sqrt{\left(\frac{Mean\ (CABV_{1S})}{Mean\ (A_1)} \times \frac{Mean\ (A_1)}{Mean(F_1)}\right)^2 \times Mean(HrHz)^2 \times (2\pi)^2 + 1}$$

$$\text{PI\_C1Ra3} = \frac{Mean(A_1)}{CPP_m} \times \sqrt{\left(\frac{Mean\ (CABV_{1S})}{Mean\ (A_1)} \times \frac{CPP_m}{FV_m}\right)^2 \times Mean(HrHz)^2 \times (2\pi)^2 + 1}$$

$$\text{PI\_C2Ra1} = \frac{Mean(A_1)}{CPP_m} \times \sqrt{\left(\frac{Mean\ (CABV_{2S})}{Mean\ (A_1)} \times \frac{ABP_m}{FV_m}\right)^2 \times Mean(HrHz)^2 \times (2\pi)^2 + 1}$$

$$\text{PI\_C2Ra2} = \frac{Mean(A_1)}{CPP_m} \times \sqrt{\left(\frac{Mean\ (CABV_{2S})}{Mean\ (A_1)} \times \frac{Mean\ (A_1)}{Mean(F_1)}\right)^2 \times Mean(HrHz)^2 \times (2\pi)^2 + 1}$$

$$\text{PI\_C2Ra3} = \frac{Mean(A_1)}{CPP_m} \times \sqrt{\left(\frac{Mean\ (CABV_{2S})}{Mean\ (A_1)} \times \frac{CPP_m}{FV_m}\right)^2 \times Mean(HrHz)^2 \times (2\pi)^2 + 1}$$

$$\mathrm{PI\_C3Ra1} = \frac{Mean(A_1)}{CPP_m} \times \sqrt{\left(\frac{Mean\ (CABV_{3S})}{Mean\ (A_1)} \times \frac{ABP_m}{FV_m}\right)^2 \times Mean(HrHz)^2 \times (2\pi)^2 + 1}$$

$$\mathrm{PI\_C3Ra2} = \frac{Mean(A_1)}{CPP_m} \times \sqrt{\left(\frac{Mean\ (CABV_{3S})}{Mean\ (A_1)} \times \frac{Mean\ (A_1)}{Mean(F_1)}\right)^2 \times Mean(HrHz)^2 \times (2\pi)^2 + 1}$$

$$\mathrm{PI\_C3Ra3} = \frac{Mean(A_1)}{CPP_m} \times \sqrt{\left(\frac{Mean\ (CABV_{3S})}{Mean\ (A_1)} \times \frac{CPP_m}{FV_m}\right)^2 \times Mean(HrHz)^2 \times (2\pi)^2 + 1}$$

where ABP_m, CPP_m, and FV_m each represent the mean value of the respective parameter, A_1 the fundamental harmonic of ABP, F_1 the fundamental amplitude of the FV waveform, $CABV_{1\text{-}3S}$ the time-averaged mean values of each ΔCaBV estimation method resolved into the spectral domain, and $HrHz$ the fundamental frequency of FV.

References

[1] Kim D-J, Kasprowicz M, Carrera E, Castellani G, Zweifel C, Lavinio A, et al. The monitoring of relative changes in compartmental compliances of brain. Physiol Meas 2009;30:647–59.

[2] Varsos GV, Richards H, Kasprowicz M, Budohoski KP, Brady KM, Reinhard M, et al. Critical closing pressure determined with a model of cerebrovascular impedance. J Cereb Blood Flow Metab 2013;33(2):235–43.

[3] Ambarki K, Baledent O, Kongolo G, Bouzerar R, Fall S, Meyer ME. A new lumped-parameter model of cerebrospinal hydrodynamics during the cardiac cycle in healthy volunteers. IEEE Trans Biomed Eng 2007;54(3):483–491.

[4] Panerai RB, Salinet ASM, Brodie FG, Robinson TG. The influence of calculation method on estimates of cerebral critical closing pressure. Physiol Meas 2011;32(4):467–82. Available from: http://stacks.iop.org/0967-3334/32/i=4/a=007?key=crossref.e5a09afc7939209a064aae0f2debd176.

[5] Czosnyka M, Smielewski P, Kirkpatrick P, Piechnik S, Laing R, Pickard JD. Continuous monitoring of cerebrovascular pressure-reactivity in head injury. Acta Neurochir Suppl. 1998;71:74–7.

[6] Calviello LA, Donnelly J, Zeiler FA, Thelin EP, Smielewski P, Czosnyka M. Cerebral autoregulation monitoring in acute traumatic brain injury: what's the evidence? Minerva Anestesiol 2017;83(8).

[7] Uryga A, Kasprowicz M, Diehl R, Kaczmarska K, Calviello L, Czosnyka M. Assessment of cerebral hemodynamic parameters using pulsatile versus non-pulsatile blood outflow model. J Clin Monit Comput 2018:1–10.

[8] Avezaat CJJ, Van Eijndhoven JHM. The role of the pulsatile pressure variations in intracranial pressure monitoring. Neurosurg Rev 1986;9:113–20.

[9] Czosnyka M, Guazzo E, Whitehouse M, Smielewski P, Czosnyka Z, Kirkpatrick P, et al. Significance of intracranial pressure waveform analysis after head injury. Acta Neurochir (Wien) 1996;138(5):531–42.

[10] Calviello LA, de Riva N, Donnelly J, Czosnyka M, Smielewski P, Menon DK, et al. Relationship between brain pulsatility and cerebral perfusion pressure: replicated validation using different drivers of CPP change. Neurocrit Care 2017 Dec 1;27(3):392–400.

[11] Steiner LA, Balestreri M, Johnston AJ, Czosnyka M, Coles JP, Chatfield DA, et al. Sustained moderate reductions in arterial CO_2 after brain trauma time–course of cerebral blood flow velocity and intracranial pressure. Intensive Care Med 2004;30(12):2180–7.

[12] Helmy A, Vizcaychipi M, Gupta AK. Traumatic brain injury: intensive care management. Br J Anaesth 2007;99:32–42.

[13] Carrera E, Kim D-J, Castellani G, Zweifel C, Czosnyka Z, Kasprowicz M, et al. What shapes pulse amplitude of intracranial pressure? J Neurotrauma Feb 2010;27(2):317–24. Available from: http://www.liebertonline.com/doi/abs/10.1089/neu.2009.0951.

[14] Avezaat C, Eijndhoven JVan. Cerebrospinal fluid pulse pressure and craniospinal dynamics: a theoretical, clinical and experimental study. Resuscitation 1984;5:111–26. Available from: http://www.ncbi.nlm.nih.gov/pubmed/1028117%5Cnhttp://repub.eur.nl/pub/38457.

[15] Risberg J, Lundberg N, Ingvar DH. Regional cerebral blood volume during acute transient rises of the intracranial pressure (Plateau waves). J Neurosurg Sep 1969;31(3):303–10.

[16] Grubb RL, Raichle ME, Eichling JO, And MM, Ter-Pogossian J. The effects of changes in $PaCO_2$ on cerebral blood volume, blood flow, and vascular mean transit time. Stroke 1974;5(5):630–9.

[17] Ito H, Kanno I, Ibaraki M, Hatazawa J, Miura S. Changes in human cerebral blood flow and cerebral blood volume during hypercapnia and hypocapnia measured by positron emission tomography. J Cerebral Blood Flow Metabol 2003;23(6):665–70.

[18] Haubrich C, Steiner LA, Diehl RR, Kasprowicz M, Smielewski P, Pickard JD, et al. Doppler flow velocity and intra-cranial pressure: responses to short-term mild hypocapnia help to assess the pressure-volume relationship after head injury. Ultrasound Med Biol 2013;39(9):1521–6.

[19] Roberts BW, Karagiannis P, Coletta M, Kilgannon JH, Chansky ME, Trzeciak S. Effects of $PaCO_2$ derangements on clinical outcomes after cerebral injury: a systematic review. Resuscitation 2015;91:32–41.

[20] Meng L, Gelb AW, Alexander BS, Cerussi AE, Tromberg BJ, Yu Z, et al. Impact of phenylephrine administration on cerebral tissue oxygen saturation and blood volume is modulated by carbon dioxide in anaesthetized patients. Br J Anaesth 2012;108(5):815–22.

[21] Sookplung P, Siriussawakul A, Malakouti A, Sharma D, Wang J, Souter MJ, et al. Vasopressor use and effect on blood pressure after severe adult traumatic brain injury. Neurocrit Care 2011;15(1):46–54.

[22] Panerai RB, Deverson ST, Mahony P, Hayes P, Evans DH. Effects of CO_2 on dynamic cerebral autoregulation measurement. Physiol Meas 1999;20(3):265–75.

[23] Minciotti P, Ceravolo MG, Provinciali L. Inter-examiner variability of transcranial Doppler procedure and reports: a multicenter survey. Italian Transcranial Doppler Group. Ital J Neurol Sci 1997;18(1):21–30. Available from: http://www.ncbi.nlm.nih.gov/pubmed/9115039.

[24] Sperna Weiland NH, Brevoord D, Jöbsis DA, de Beaumont EMFH, Evers V, Preckel B, et al. Cerebral oxygenation during changes in vascular resistance and flow in patients on cardiopulmonary bypass – a physiological proof of concept study. Anaesthesia 2017;72(1):49–56.

[25] Czosnyka M, Guazzo E, Whitehouse M, Smielewski P, Czosnyka Z, Kirkpatrick P, et al. Significance of intracranial pressure waveform analysis after head injury. Acta Neurochir (Wien) 1996;138(5):531–42. Available from: http://link.springer.com/10.1007/BF01411173.

[26] De Riva N, Budohoski KP, Smielewski P, Kasprowicz M, Zweifel C, Steiner LA, et al. Transcranial doppler pulsatility index: what it is and what it isn't. Neurocrit Care 2012;17(1):58–66.

[27] Kasprowicz M, Czosnyka M, Soehle M, Smielewski P, Kirkpatrick PJ, Pickard JD, et al. Vasospasm shortens cerebral arterial time constant. Neurocrit Care 2012;16(2):213–18.

[28] Richards HK, Czosnyka M, Whitehouse H, Pickard JD. Increase in transcranial Doppler pulsatility index does not indicate the lower limit of cerebral autoregulation. Acta Neurochir Suppl 1998;71:229–32. Available from: http://www.ncbi.nlm.nih.gov/entrez/query.fcgi?cmd=Retrieve&db=PubMed&dopt=Citation&list_uids=9779192.

[29] Brothers RM, Zhang R. CrossTalk opposing view: the middle cerebral artery diameter does not change during alterations in arterial blood gases and blood pressure. J Physiol 2016;594:4077–9.

[30] Hoiland RL, Ainslie PN. CrossTalk proposal: the middle cerebral artery diameter does change during alterations in arterial blood gases and blood pressure. J Physiol 2016;594:4073–5.

[31] Carney N, Totten AM, O'Reilly C, Ullman JS, Hawryluk GWJ, Bell MJ, et al. Guidelines for the management of severe traumatic brain injury, fourth edition. Neurosurgery 2017;80(1):6–15.

[32] Sorrentino E, Diedler J, Kasprowicz M, Budohoski KP, Haubrich C, Smielewski P, et al. Critical thresholds for cerebrovascular reactivity after traumatic brain injury. Neurocrit Care 2012;16(2):258–66.

[33] Brady KM, Lee JK, Kibler KK, Easley RB, Koehler RC, Shaffner DH. Continuous measurement of autoregulation by spontaneous fluctuations in cerebral perfusion pressure: comparison of 3 methods. Stroke 2008;39(9):2531–7.

[34] Zeiler FA, Donnelly J, Smielewski P, Menon DK, Hutchinson PJ, Czosnyka M. Critical thresholds of intracranial pressure-derived continuous cerebrovascular reactivity indices for outcome prediction in noncraniectomized patients with traumatic brain injury. J Neurotrauma 2018 May 15;35(10):1107–15.

[35] Steiner LA, Czosnyka M, Piechnik SK. Continuous monitoring of cerebrovascular pressure reactivity allows determination of optimal cerebral perfusion pressure in patients with traumatic brain injury. Crit Care 2002;30(4):733–8.

[36] Aries MJH, Czosnyka M, Budohoski KP, Steiner LA, Lavinio A, Kolias AG, et al. Continuous determination of optimal cerebral perfusion pressure in traumatic brain injury. Crit Care Med 2012;40(8):2456–63.

[37] Needham E, McFadyen C, Newcombe V, Synnot AJ, Czosnyka M, Menon D. Cerebral perfusion pressure targets individualized to pressure-reactivity index in moderate to severe traumatic brain injury: a systematic review. J Neurotrauma 2017;34(5):963–70.

[38] Lazaridis C, DeSantis SM, Smielewski P, Menon DK, Hutchinson P, Pickard JD, et al. Patient-specific thresholds of intracranial pressure in severe traumatic brain injury. J Neurosurg 2014;120(4):893–900. Available from: http://thejns.org/doi/10.3171/2014.1.JNS131292.

[39] Kasprowicz M, Diedler J, Reinhard M, Carrera E, Smielewski P, Budohoski KP, et al. Time constant of the cerebral arterial bed. Acta Neurochirurgica, Supplementum 2012:17–21.
[40] Horikoshi T, Akiyama I, Yamagata Z, Sugita M, Nukui H. Magnetic resonance angiographic evidence of sex-linked variations in the circle of willis and the occurrence of cerebral aneurysms. J Neurosurg 2002;96(4):697–703.
[41] Ito H, Ibaraki M, Kanno I, Fukuda H, Miura S. Changes in the arterial fraction of human cerebral blood volume during hypercapnia and hypocapnia measured by positron emission tomography. J Cereb Blood Flow Metab 2005;25:852–7.
[42] Steiner LA, Coles JP, Johnston AJ, Chatfield DA, Smielewski P, Fryer TD, et al. Assessment of cerebrovascular autoregulation in head-injured patients: a validation study. Stroke 2003;34(10):2404–9.